

Adaptive Control of Robotic Surface Finishing Processes

Prabhakar R. Pagilla* and Biao Yu

School of Mechanical and Aerospace Engineering
Oklahoma State University
Stillwater, OK 74078-5016

Abstract

Adaptive control of robotic surface finishing processes such as deburring, grinding, chamfering and polishing is considered in this paper. In the authors prior work, a dynamic model that describes the behavior of the robot for a complete surface finishing task was developed. We also developed a control scheme that enables stable transition of the robot from free motion to constrained motion on the surface. In this paper, emphasis is given to the constrained motion on the surface that includes motion control along the surface and force control normal to the surface. The focus of the paper is on two aspects. First, adaptation of the grinding coefficient that relates the normal and the tangential force on the surface is studied. Second, two types of constraint surfaces, straight and curved, are considered in the study. Experiments were conducted for a complete robot task for both types of surfaces. Experimental results show good tracking performance for both the surfaces with the proposed adaptive control design. Further, convergence of the grinding coefficient to a constant for both surfaces is observed.

1 Introduction

Conventional machine tools, such as CNC operated, are used in general to remove large amount of material to shape a part to its desired geometry. Finishing of the machined part is required to remove material in small amounts to bring the part to the required tolerance. In addition to small material removal, localized burr formations have to be removed. Examples of these surface finishing operations are grinding, deburring, and chamfering. These operations constitute a significant portion of effort and money in the manufacturing industry. Automation of such processes is still in its rudimentary stages.

It is known that material finishing operations such as deburring, grinding, chamfering and other edge finishing operations can be responsible for 10 to 30 percent of all manufacturing costs [1, 2]. Automation of surface finishing operations is an active area of investigation in the manufacturing industry and also in several national laboratories, including the National Institute of Standards and Technology and Sandia National Laboratories. Several important research prob-

lem areas have been pointed out in [1]. Accurate position and force control of the robot in the presence of uncertainties and stable transition between free motion and contact motion were reported to be some of the major factors that need to be addressed to create an advanced deburring system. In [4] experimental results for robotic deburring of two-dimensional parts using an impedance control method have been shown. Deburring using force control and active end-effector system has been presented in [19].

Considerable research in the theory of constrained mechanical systems has been reported in the last decade, see [3] and its references. Some of the early work on simultaneous position and force control of robot manipulators was done in [5, 6]. The motivation for some of this early work was to make progress towards automation of manually performed manufacturing operations. Precise positioning of the robot relative to the workpiece is required for efficiently performing these operations. Force feedback is often used to compensate for positioning inaccuracies. Control algorithms that emerged in this area during the 80's and 90's can be broadly classified into three categories: hybrid position/force control [7]; impedance control [8]; and constrained mechanical systems modeled as differential-algebraic equations [3, 11].

The authors prior work focused on development of a dynamic model and a stable transition controller design for constrained robots [9]. In this work, we focus on the constrained motion phase. At steady feed-rate (velocity tangential to the surface) the normal force magnitude and tangential force magnitude are related by coefficient of grinding friction [17]. It is crucial to have a good estimate of this coefficient to obtain a better surface finish. In this paper we propose an adaptive control algorithm for the constrained motion phase which involves on-line estimation of the grinding coefficient. Extensive experiments were conducted with the proposed adaptive control design. Most prior experimental work in literature has focused on the straight constraint surface. In this paper, experiments were conducted for both straight and curved surfaces. In the case of curved surfaces, the normal direction of the constraint surface is varying as the robot end-effector moves on the surface as opposed to the straight surface. This creates added problems of keeping the robot end-effector on the curved surface. The proposed adaptive controller achieves good tracking along the surface and force regulation normal to the surface. Most prior experimental work in literature

*Corresponding author: pagilla@ceat.okstate.edu

has assumed that the robot is in contact with the surface. In this paper, all the experiments are for a complete robot task, that is the robot is in free motion before making contact with the surface.

The rest of the paper is organized as follows. In Section 2, we describe the dynamic model of the robot for surface finishing operations. Control algorithms for each phase of the complete task are given in Section 3. Section 4 gives a description of the experimental platform. Experimental results for both straight and curved surfaces are discussed in Section 5. Section 6 gives conclusions and future research.

2 Dynamic Model for Surface Finishing Operations

Let the kinetic and potential energy functions of an n -link robot be given by $\mathcal{K}(q, \dot{q}) = \frac{1}{2} \dot{q}^T M(q) \dot{q}$ and $\mathcal{P}(q)$, where q, \dot{q} are the generalized position and velocity, respectively, and $M(q) \in \mathbb{R}^{n \times n}$ is the symmetric positive definite mass matrix. The dynamics of the robot is given by

$$M(q)\ddot{q} + C(q, \dot{q})\dot{q} + g(q) = \tau + J^T(q)f \quad (1)$$

where $C(q, \dot{q}) \in \mathbb{R}^{n \times n}$ is the matrix composed of Coriolis and centripetal terms, $g(q)$ is the gravity vector, τ is the vector composed of motor torque applied at each joint of the robot, f represents the vector of external forces, and $J(q)$ is the Jacobian of the manipulator. Let the geometric constraint on the robot be modeled by the unilateral constraint

$$\phi(x(q)) \leq 0, \quad (2)$$

where $x(q)$ is the Cartesian position. The constraint is assumed to be smooth. Define the following orthogonal projection matrix, whose image represents the normal direction of the constraint,

$$P_\phi(q) = (\nabla\phi_q(q)) (\nabla\phi_q(q))^T / \|\nabla\phi_q(q)\|^2 \quad (3)$$

where $\|\cdot\|$ denotes the 2-norm. The kernel of $P_\phi(q)$ gives the tangential direction of the constraint, and is given by $Q_\phi(q) = I - P_\phi(q)$. The external force f is the contact force and can be written as

$$f = n(x(q))f_n + t(x(q))f_t \quad (4)$$

where $n(x(q))$ and $t(x(q))$ represent the unit normal and tangential directions of the constraint surface, respectively, in the Cartesian space, and f_n and f_t represent the normal force and tangential force magnitude, respectively. A complete task of the robot in the presence of the unilateral constraint can be divided into three phases: (a) if $\phi(q) < 0$, then the robot is said to be in free motion phase, (b) if $\phi(q) = 0$ and the velocity normal to the surface is zero, then the robot is said to be in the constrained motion phase, and (c) if $\phi(q) = 0$ and the velocity normal to the surface is non-zero, then the robot end-effector has a tendency to bounce on the surface, and it is said to be in the transition phase. The transition phase begins with the first contact of the robot with the surface and lasts until the velocity normal to the surface becomes zero.

During the constrained motion phase, it is known that when steady contact and feedrate (velocity along the constraint surface) is reached, f_n and f_t are related by the coefficient of grinding friction [17], that is,

$$f_t = \xi f_n \quad (5)$$

where ξ is the coefficient of grinding friction. The robot dynamics during surface finishing process becomes

$$M(q)\ddot{q} + C(q, \dot{q})\dot{q} + g(q) = \tau + v(q)f_n + v'(q)\xi f_n \quad (6)$$

where $v(q) := J^T(q)n(x)$ and $v'(q) := J^T(q)t(x)$. Notice that $v(q)$ and $v'(q)$ map the normal force and the tangential force magnitude, respectively, into corresponding joint forces. The dynamics for a complete surface finishing task is summarized below.

- Unconstrained motion phase:

$$M(q)\ddot{q} + C(q, \dot{q})\dot{q} + g(q) = \tau \quad (7)$$

- Transition phase:

$$M(q)\ddot{q} + C(q, \dot{q})\dot{q} + g(q) = \tau \quad \text{and} \quad \dot{q}_+ = \mathcal{D}(q, \dot{q}_-) \quad (8)$$

- Constrained motion phase:

$$M(q)\ddot{q} + C(q, \dot{q})\dot{q} + g(q) = \tau + v(q)f_n + v'(q)\xi f_n \quad (9)$$

The second term in (8) gives an impact model for the surface. This impact model relates the post-impact velocity to the pre-impact velocity. We assume the existence of an impact model that incorporates kinetic energy reduction of the robot during impact. Detailed discussion of the impact models and transition phase can be found in [10, 9].

3 Control Design

For surface finishing operations, the control goal is to move the robot towards the surface, make contact with the surface, perform the designed operation, i.e., chamfering, deburring, polishing, etc., and leave the surface to return to the initial point. The desired motion trajectories are designed based on the location of the surface with respect to the robot. During the constrained motion phase, the robot end-effector follows the surface while applying a desired force normal on the surface. The control goal in the unconstrained motion phase is to track the desired motion trajectory considering manipulator model uncertainties. During the constrained motion phase, the control goal is to simultaneously track the desired motion in tangential direction and regulate the desired force normal to the constraint surface. Switching directly to simultaneous motion and force control in the constrained motion could lead to repeated impacts of the robot end-effector on the surface. A stable transition controller assures that repeated impacts do not occur. In the following control law for each phase is given.

3.1 Adaptive control during the unconstrained phase

In this phase, an experimentally well tested model-based adaptive controller considering robot parameter uncertainties is chosen. The adaptive model-based control law and parameter adaptation law are

$$\tau = Y(q, \dot{q}, \ddot{q}_r) \hat{\beta}(t) - F_v e_v(t) \quad (10)$$

$$\hat{\beta}(t) = \beta_0 - \int_0^t \Gamma^{-T} Y^T(q, \dot{q}, \ddot{q}_r) e_v(\omega) d\omega \quad (11)$$

where $\dot{q}_r := \dot{q}_d - \Lambda_p e$, $e = q - q_d$, $e_v = \dot{q} - \dot{q}_r$, F_v , Γ , Λ_p are positive definite gain matrices, $\hat{\beta}(t)$ and β_0 are the estimate and initial known value of β , respectively, and

$$Y(q, \dot{q}, \ddot{q}_r) \hat{\beta}(t) = \widehat{M}(q) \ddot{q}_r + \widehat{C}(q, \dot{q}) \dot{q}_r + \widehat{g}(q).$$

Substituting the control law (10) into the free motion robot dynamics (7) and rearranging terms results in the following error dynamics

$$M(q) \dot{e}_v + C(q, \dot{q}) e_v + F_v e_v = Y(q, \dot{q}, \ddot{q}_r) \tilde{\beta}(t) \quad (12)$$

where $\tilde{\beta}(t) = \hat{\beta}(t) - \beta$ is the parameter estimation error.

3.2 Discontinuous control during the transition phase

Transition phase starts when the robot makes its first impact with the surface. Then, we project the desired trajectory into tangential direction of the surface using the tangential projection matrix Q_ϕ . The desired motion trajectory of the robot is developed based on apriori knowledge of the location of the constraint. The first impact gives the actual location of the constraint surface. After the first impact, the desired trajectory is modified such that the desired velocity and acceleration in normal direction are zero, i.e., $P_\phi \dot{q}_d = 0$. The control law for the transition phase is chosen as follows:

$$\tau = Y(q, \dot{q}, \ddot{q}_r) \beta - F_v e_v - \lambda_{tn} P_\phi \operatorname{sgn}(e_{vn}) \quad (13)$$

where $\dot{q}_r = \dot{q}_d - \lambda_p e = Q_\phi \dot{q}_d - \lambda_p e$, $e_v = \dot{q} - \dot{q}_r$, $e_{vn} = P_\phi e_v$, and λ_{tn} , λ_p are positive gains. Substituting the control law into the dynamic equations we obtain the error dynamics

$$M(q) \dot{e}_v + C(q, \dot{q}) e_v + F_v e_v + \lambda_{tn} P_\phi \operatorname{sgn}(e_{vn}) = 0 \quad (14)$$

3.3 Adaptive motion/force control during the constrained phase

When the transition phase dies down, i.e., the velocity normal to the surface becomes zero ($P_\phi \dot{q} \rightarrow 0$), then the robot is in stable contact with the surface. At this time we switch to constrained motion control, i.e., motion control in the tangential direction and force control in the normal direction. In this phase it is assumed that the inertial parameters of the robot are estimated during the free motion phase and hence known. We choose the following control law and

estimation law for the grinding coefficient

$$\tau = M(q) \ddot{q}_r + C(q, \dot{q}) \dot{q}_r - F_v e_v - v(q) f_{nd} - v'(q) \hat{\xi} f_n \quad (15)$$

$$\dot{\hat{\xi}} = -\gamma_f v'^T(q) e_v f_n \quad (16)$$

where f_{nd} is the desired normal force, $e_{fn} = f_n - f_{nd}$, $e_v = \dot{q} - \dot{q}_r$, and

$$\begin{aligned} \dot{q}_r &= Q_\phi [\dot{q}_d - \Lambda_p e] + \beta_f \bar{v}(q) e_{vfn} \\ \bar{v}(q) &= v(q) / \|v(q)\|^2 \\ e_{vfn} &= \int_0^t e_{fn}(\omega) d\omega \end{aligned}$$

Substituting the control law (15) into the dynamic equation (9) we obtain

$$M(q) \dot{e}_v + C(q, \dot{q}) e_v + F_v e_v = v(q) e_{fn} + v'(q) \tilde{\xi} f_n \quad (17)$$

where $\tilde{\xi} = \hat{\xi} - \xi$ is the estimation error of the grinding coefficient.

An event based control switching strategy is developed for the complete task. The desired motion trajectory is generated based on apriori knowledge of the location of the constraint. In the event of impact, this desired trajectory is projected into the tangential directions of the constraint surface. The actual location of the constraint surface is known after the first impact. Regulation problem is considered in the normal direction, i.e., regulation of the tool onto the surface with zero normal velocity. Notice that the reference velocity error, e_v , in each phase is different, even though we use the same notation for it in each phase. The closed-loop system is shown to be stable within each phase and the robot system states are bounded when switching from one phase to another. Stability of the control algorithm for the complete task including individual phases can be found in [10].

4 Experiments

The robotic surface finishing system consists of a two-link robot system, computer for real-time control, force sensor, surface finishing tool, and a constraint fixture. Figure 1 illustrates the complete hardware platform of the robotic surface finishing system. The main part of the system is a

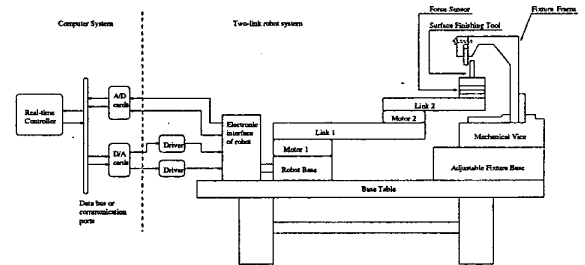


Figure 1: Schematic of the Robotic Surface Finishing System two-axis direct drive manipulator, which is shown in Figure

1. Each axis is driven by an NSK Megatorque direct drive servo-motor. Details of the experimental platform and the dynamic model of the manipulator can be found in [10].

Experiments were conducted with two types of constraint surfaces, i.e., straight and curved. Fig. 2 shows the desired trajectories of the robot interacting with straight and curved surfaces. The straight surface is a thick straight aluminum

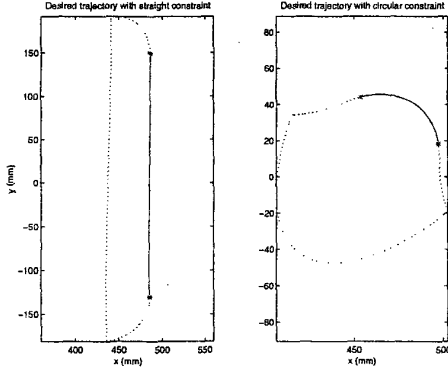


Figure 2: Robot Desired Trajectory

sheet and the curved surface is a cylindrical steel workpiece. Both constraint surfaces are held firmly by vice as shown in Fig. 1. In Fig. 2, the dotted lines represent the unconstrained motion path of the robot and the solid lines correspond to the constrained motion path. Therefore, the desired complete task of the robot is to move towards the constraint surface, make contact with the surface, follow the surfaces while maintaining a desired normal contact force, and leave the surfaces to return to the starting point. In Cartesian coordinates, the straight and the circular constraint surfaces and their gradients are given by

$$y - mx = c \quad (18)$$

$$(x - a)^2 + (y - b)^2 = r^2 \quad (19)$$

where x, y represent the Cartesian coordinates, and m, c, a, b, r are constant parameters. It should be noted that the gradient of the straight surface, (18), is the vector $[-m, 1]$, whereas the gradient of the circular surface is the vector $[x - a, y - b]$. Therefore, the tracking error tangential to the surface affects the gradient of the circular surface, whereas the tangential tracking error has no effect on the gradient of the straight surface. Since the work parts generally contain a combination of straight and curved surfaces on them, it is necessary that the designed control algorithm perform well for both cases. The proposed adaptive control algorithm performs equally well for both types of surfaces, and hence can be used for a wide variety of work parts.

The desired trajectories shown in Fig. 2 are designed such that without any uncertainty in the location of the constraint, the robot lands on the surfaces smoothly, i.e., there is no normal velocity at contact. The desired velocity of

the robot end-effector in Cartesian coordinates during constrained motion is chosen to be a constant to mimic steady feed-rate during surface finishing. Also, the desired trajectories are such that the entire task is completed in 12 seconds for the straight surface and 10 seconds for curved surface. The desired normal force during constrained motion phase is chosen to be 35 N. Control sampling period of 4 milli-seconds and force data sampling period of 0.5 milli-seconds is used in all the experiments. Higher force sampling frequency reduces time-delay introduced due to force data filtering.

To better illustrate the performance of the controller during constrained motion, the tracking errors shown are the Cartesian position tracking errors projected into the frame on the constraint surface. Fig. 3 shows the normal and tangential tracking errors for the straight surface. In the figure, the start and end of the constrained motion phase, respectively, are denoted by small circles at the six second and ten second time instant. Observe that the friction between the robot end-effector and the surface causes tangential tracking error during the constrained motion phase. Fig. 4 shows the normal and tangential force on the constraint surface. Fig. 5 and Fig. 6 represent the position tracking errors and the force signals for the experiments with the circular surface. Since the constraint surface is circular, the desired normal force vector is a vector with constant magnitude and varying direction.

In practical situations, it is difficult to obtain the value of grinding coefficient because this value depends on a number of aspects such as material of the surface, feedrate, grain size of the tool, etc. Typically most of these conditions are fixed for a particular surface finishing process and the work part. In a very broad sense it can be assumed that the normal and tangential forces are related by an unknown constant, typically known as the grinding friction coefficient [17]. An adaptation law to estimate the coefficient of grinding friction on-line was proposed in this paper. Fig. 7 and Fig. 8 are the on-line estimates of the grinding friction coefficient with straight and circular surfaces, respectively. These figures show experimental results with various initial values and adaptation gains. The results show that the estimates of the grinding coefficient converge to constant values regardless of their assumed initial values and adaptation gains. In Fig. 7, the estimate converges in five cycles of the desired trajectory with an adaptation gain of $\gamma_f = 0.1$, whereas the estimate converges in four cycles with a gain of $\gamma_f = 0.3$. Similarly, in Fig. 8, the estimate converges in six cycles of the desired trajectory with an adaptation gain of $\gamma_f = 0.3$, whereas the estimate converges in four cycles with a gain of $\gamma_f = 0.5$. Since the material of the straight surface is aluminum and the circular surface is steel, it should be observed that the converged value of the grinding friction coefficient is different for the straight and circular surface.

Further, to better illustrate the performance of the proposed adaptive control design, Fig. 9 and Fig. 10 show the L_2 norm of the normal and tangential tracking errors for straight and circular surfaces, respectively, during the con-

strained motion phase. Observe that the L_2 norm of tangential position tracking error improves after each cycle as a result of the improvement in the estimate of the grinding coefficient.

5 Conclusions

In this paper, we proposed an adaptive control design for robot manipulators performing surface finishing operations. Emphasis was given to the constrained motion phase, especially to the estimation of the grinding coefficient of friction. Extensive experiments were conducted to show that the proposed design gives good performance without a good knowledge of the grinding friction coefficient. The on-line estimate of the grinding coefficient converges to a constant value irrespective of the initial values and adaptation gains for both the surfaces.

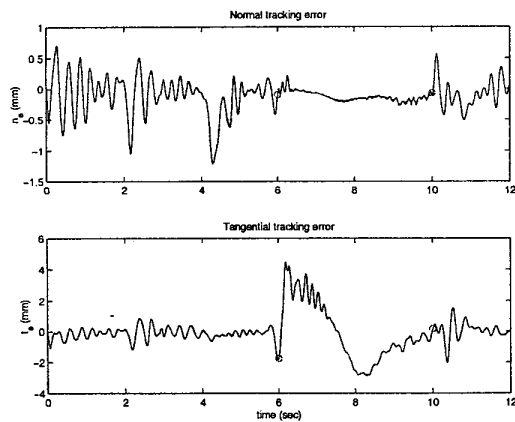


Figure 3: Tracking errors, straight surface

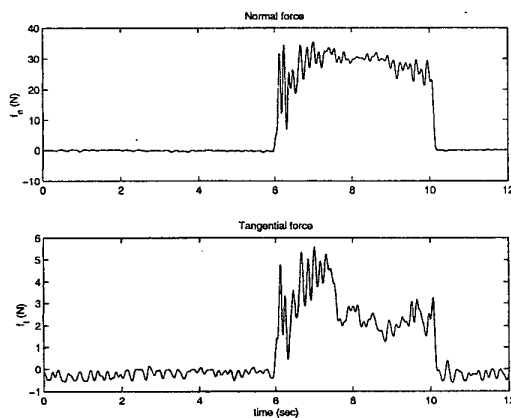


Figure 4: Normal and tangential force, straight surface

References

[1] N. Ramachandran, N. Pande, and N. Ramakrishnan, "The Role of Deburring in Manufacturing: A State-of-the-Art Survey," *Journal of Materials Processing Technology*, vol. 44, 1994.

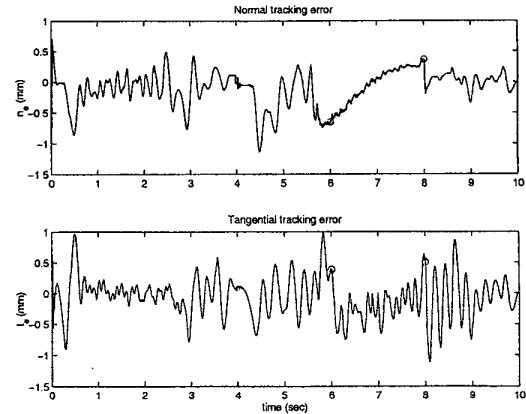


Figure 5: Tracking errors, circular surface

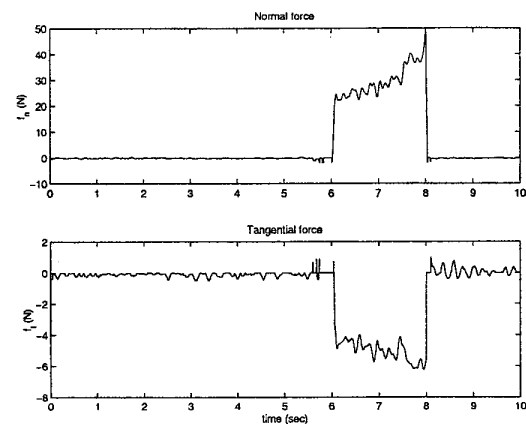


Figure 6: Normal and tangential force, circular surface

[2] R. Komanduri, M.E. Merchant, and M.C. Shaw, "Symposium on US Contributions to Machining and Grinding Research in the 20th Century," *Applied Mechanics Reviews*, vol. 46, no. 3, 1993.

[3] S. Arimoto, *Control theory of non-linear mechanical systems - a passivity-based and circuit-theoretic approach*. Oxford Univ. Press Inc., New York, 1996.

[4] H. Kazerooni, "Robotic Deburring of Two-dimensional Parts with Unknown Geometry," *Journal of Manufacturing Systems*, vol. 7, no. 4, pp. 329-338, 1988.

[5] D.E. Whitney, "Force Feedback Control of Manipulators," *ASME Journal of Dynamic Systems, Measurement and Control*, vol. 102, pp. 91-97, 1977.

[6] M.H. Raibert and J.J. Craig, "Hybrid Position/Force Control of Manipulators," *ASME Journal of Dynamic Systems, Measurement and Control*, vol. 102, pp. 126-133, 1981.

[7] M.T. Mason, "Compliance and Force Control of Computer Controlled Manipulators," *IEEE Trans. on System, Man and Cybernetics*, SMC-11(6), pp. 418-432, 1981.

[8] N. Hogan, "Impedance Control: An approach to manipulation: Part I-Theory; Part II - Implementation; Part III - Appli-

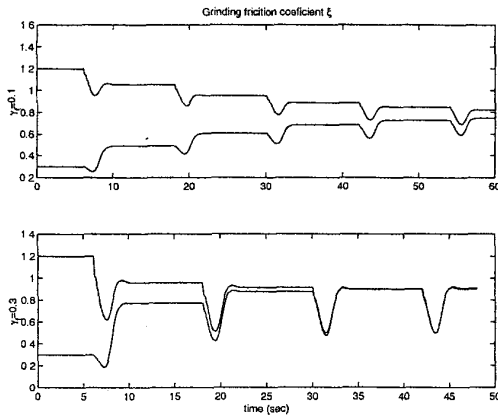


Figure 7: Grinding coefficient estimate, straight surface

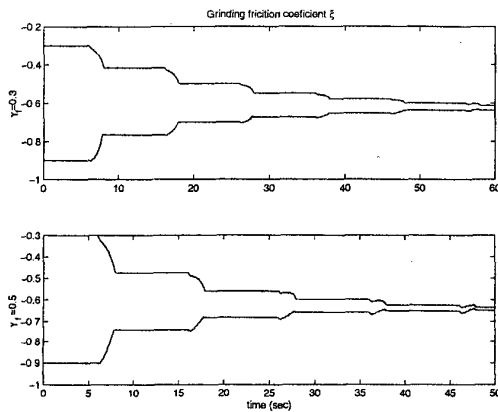


Figure 8: Grinding coefficient estimate, circular surface

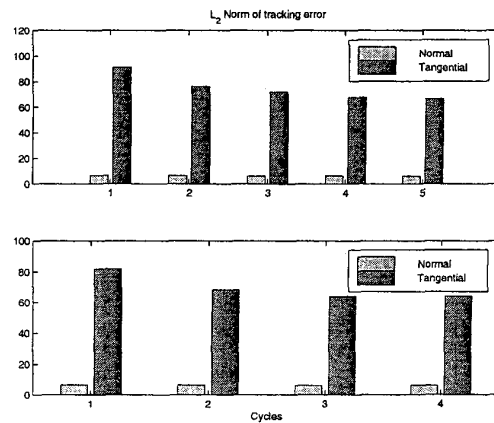


Figure 9: L_2 norm of tracking error, straight surface

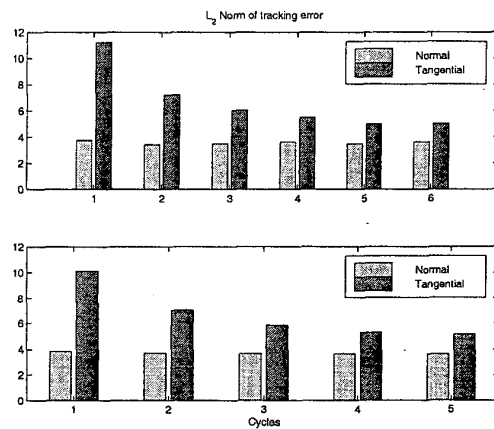


Figure 10: L_2 norm of tracking error, circular surface

cations," *ASME Journal of Dynamic Systems, Measurement and Control*, vol. 107, pp. 1–24, 1985.

[9] P.R. Pagilla and B. Yu, "A Stable Transition Controller for Constrained Robots," *IEEE/ASME Trans. on Mechatronics*, vol. 6, no. 1, pp. 1–13, March 2001.

[10] B. Yu, "Modeling, Control Design, and Mechatronic Implementation of Constrained Robots for Surface Finishing Applications," Ph.D. thesis, Oklahoma State University, Stillwater, OK, December 2000.

[11] D. Wang and N.H. McClamroch, "Position and Force Control for Constrained Manipulator Motion: Lyapunov's Direct Method," *IEEE Trans. on Robotics and Automation*, vol. 9, no. 3, pp. 308–312, 1993.

[12] Mills, J.K., and Lokhorst, D.M., 1993, "Stability and Control of Robotic Manipulators During Contact/Noncontact Task Transition," *IEEE Trans. on Robotics and Automation*, vol. 9, No. 3, pp. 335–346.

[13] K. Youcef-Toumi and D.A. Gutz, "Impact and Force Control: Modeling and Experiments," *ASME Journal of Dynamic Systems, Measurement and Control*, pp. 89–98, 1994.

[14] P.R. Pagilla and M. Tomizuka, "Contact Transition Control of Nonlinear Mechanical Systems Subject to a Unilateral Con-

straint," *ASME Journal of Dynamic Systems, Measurement and Control*, vol. 119, pp. 749–759, 1997.

[15] T.J. Tarn, Y. Wu, N. Xi, and A. Isidori, "Force Regulation and Contact Transition Control," *IEEE Control Systems Magazine*, pp. 32–40, February, 1996.

[16] B. Brogliato, S. Niculescu, P. Orhant, "On the control of finite dimensional mechanical systems with unilateral constraints," *IEEE Trans. on Automatic Control*, vol. 42, no. 2, pp. 200–215, 1997.

[17] R. King and R. Hahn, *Handbook of Modern Grinding Technology*. Chapman and Hall, 1986.

[18] L.L. Whitcomb and S. Arimoto, "Adaptive Model-Based Hybrid Control of Geometrically Constrained Robot Arms," *IEEE Trans. on Robotics and Automation*, vol. 13, no. 1, pp. 105–116, 1997.

[19] G.M. Bone, M.A. Elbestawi, R. Lingarkar, and L. Liu, "Force Control of Robotic Deburring," *ASME Journal of Dynamic Systems, Measurement and Control*, vol. 113, 1991.